Journal of Alloys and Compounds 408–412 (2006) 1078–1083

Journal of ALLOYS AND COMPOUNDS

www.elsevier.com/locate/jallcom

Oxidation behavior of reduced $(CeO_2)_{1-x}$-$(ZrO_2)_x$ ($x = 0, 0.2, 0.5$) catalysts

Noriyoshi Kakuta*, Satoshi Ikawa, Takeshi Eguchi, Keisuke Murakami,
Hironobu Ohkita, Takanori Mizushima

Department of Materials Science, Toyohashi University of Technology,
Tempaku-cho, Toyohashi, 441-8580 Japan

Received 30 July 2004; received in revised form 6 December 2004; accepted 15 December 2004

Abstract

Oxidation properties of CeO_2-ZrO_2 catalysts were investigated as a function of oxidation temperature by a combination of TPR and O_2 pulse injection methods. Ce^{3+} species formed from the CeO_2 phase in the CeO_2-ZrO_2(5/1) catalyst and CeO_2 were very sensitive to oxygen and the amount of oxygen stored was reproducible by the oxidation at temperatures as low as 373 K. However, Ce^{3+} species formed in the solid solution of the CeO_2-ZrO_2(1/1) catalyst were relatively stable. The formation of solid solution facilitated the reducibility of Ce^{4+} species at low temperature. It was speculated from the titration profile that there were a few steps to oxidize Ce^{3+} species distributed from surface to bulk in the CeO_2-ZrO_2(1/1) catalyst.

Keywords: Cerium oxide; Zirconium oxide; Oxygen storage; Temperature programmed reduction (TPR)

---

1. Introduction

Since the strict regulations of emission level on automobile exhaust gases have been required for the environmental protection, the efforts to develop a new catalyst system for the operation under hard conditions have been continuing. Cerium oxide is well known as one of essential materials for automotive exhaust catalysts [1]. The major role of cerium oxide in the catalysts is to control of oxygen concentration by storage and release under the reaction environment. This property is so-called oxygen storage capacity (OSC). Now, in order to achieve the low emission level by the catalytic reduction, further OSC performance has been expected under operation conditions at either lower or higher temperatures.

The CeO_2–Al_2O_3 system has been widely used as the components in commercial catalysts to operate automotive three-way catalysts (TWCs) for long period; cerium oxide contributed to the thermal stability of alumina support at higher temperatures and the widening the window at temperatures of catalytic operation. From our temperature programmed reduction (TPR) study [2–6], cerium oxides on alumina was found to react with alumina at temperatures above 1173 K under the reduction condition and the $CeAlO_3$ phase formed did not restore to the initial CeO_2–Al_2O_3 system except for the oxidation at temperatures as high as 1173 K. This property induces the decrease of surface area of the catalyst and the deteriorating OSC below 1173 K because the reduced Ce^{3+} species in $CeAlO_3$ are never oxidized at lower temperatures such as 773 K. This, indeed, is the barrier to the improvement of OSC on CeO_2–Al_2O_3 systems under hard conditions required. It was necessary to develop new CeO_2 related materials instead of CeO_2–Al_2O_3.

CeO_2-ZrO_2, on which attention has been currently focused, was developed as excellent oxygen storage materials [7,8]. The formation of CeO_2-ZrO_2 solid solution leaded

---

* Corresponding author. Tel.: +81 532 44 6794; fax: +81 532 48 5833.
E-mail address: kakuta@tutms.tut.ac.jp (N. Kakuta).

0925-8388/$ – see front matter © 2005 Elsevier B.V. All rights reserved.
doi:10.1016/j.jallcom.2004.12.134

to enhance greatly reducibility of CeO_2. Structural modifications of CeO_2 lattice by the insertion of Zr^{4+} ions were suggested to be responsible for the unique reducibility behavior of CeO_2-ZrO_2 solid solution. This is explained as the generation of highly mobile lattice oxygen with the increase of distortion of the symmetry of the M–O bonds by the formation of solid solution. In addition, the advantage of CeO_2-ZrO_2 solid solution is to maintain the reversible Ce^{3+}/Ce^{4+} redox property at lower temperatures even after exposure to the reduction condition above 1173 K. Thus, most of studies were focused on the preparation of solid solutions with different Ce/Zr ratios and the evaluation of redox behavior correlated closely with OSC [9–20]. In fact, the practical use is expected as the advanced TWCs. However, although the improvement of OSC by the solid solution structure has been widely accepted, it is also evident that the behavior of OSC is strongly influenced by several factors in the preparation procedure of CeO_2-ZrO_2 such as starting material, temperature, atmosphere, kind of additive etc.

In the present work, oxidation properties of CeO_2-ZrO_2 catalysts with molar ratios of 1/1 and 5/1 were evaluated by the combination of O_2 pulse injection and TPR methods. From sequentially cyclic TPR-oxidation analyses, the CeO_2-ZrO_2 catalysts were easily oxidized as low as 373 K, suggesting the high reactivity of Ce^{3+} species with oxygen. The titration profiles with 5 ml of 1 vol.% O_2/He pulse at 773 K after TPR up to 1273 K provided the oxidation behavior of the CeO_2-ZeO_2 catalysts and CeO_2. The Ce^{3+} formed was very sensitive to oxygen on those samples. The oxygen consumption per mol-CeO_2 was improved by the formation of solid solution phase. It was presumed that the solid solution phase prevented the sintering at 1273 K and the resulting small crystallite size promoted effectively the increase of mobile oxygen estimated as OSC at 773 K.

2. Experimental

2.1. Catalyst preparation

CeO_2-ZrO_2 catalysts were prepared by a co-precipitation method. Briefly, appropriate amounts of $Ce(NO_3)_3 \cdot 6H_2O$ (Kishida Chemical) and $ZrO(NO_3)_2 \cdot 2H_2O$ (Kishida Chemical) were dissolved in a distilled water, and then ammonia solution (3%) was poured into the mixed solution under stirring. The precipitates were dried at 383 K for 24 h, followed by the calcination at 773 K for 5 h. The molar ratios of CeO_2/ZrO_2 prepared were 1/1 and 5/1. The catalysts were named CeO_2-ZrO_2(1/1) and CeO_2-ZrO_2(5/1), respectively. CeO_2 (BET surface area of $130\,m^2 g^{-1}$) powder was also employed for comparison.

2.2. Structure of CeO_2-ZrO_2 catalysts

Structure of CeO_2-ZrO_2 catalysts was examined by X-ray diffraction (XRD, RIGAKU RINT 2000) using Cu Kα radiation at 30 kV and 20 mA. Line broadening was used for the determination of the crystallite sizes.

2.3. Temperature programmed reduction (TPR) measurements

In order to characterize the oxidation behavior on those catalysts, TPR measurements were carried out up to 1273 K with a heating rate of $10\,K\,min^{-1}$. During the measurements 10 vol.% H_2/Ar was introduced into the reactor with a flow rate of $100\,ml\,min^{-1}$. The consumption of H_2 was recorded by using an on-line gas chromatograph (Shimadzu GC-8A) equipped with a thermal conductivity detector (TCD). The oxidation behavior of the reduced CeO_2-ZrO_2 catalyst was investigated in the following manner. A first TPR run was carried out using 0.25 g of the catalyst placed in the reactor without any treatments (fresh). Next the catalyst was cooled to room temperature in a stream of H_2/Ar, and then the catalyst was consecutively oxidized at desired temperatures (e.g. 773 K) for 1 h in a stream of 10 vol.% O_2/He. Finally, TPR was carried out again. The measurements were repeated at 573 and 373 K, respectively. The TPR profile comprises the amount of oxygen stored at temperatures below 773 K when the catalyst was reduced. If the reactivity with oxygen is low, i.e. the Ce–O bonding is strengthened after the consecutive oxidation, the peak area of TPR will decrease. The stability of Ce^{3+} in different oxidation temperatures can be estimated, too.

Those measurements (TPR–oxidation–TPR) were iterated at different oxidation temperatures. It should be pointed out that the experiment is performed without the exposure to air and without the replacement of the catalyst on repeated runs. In the experimental condition, the reproducibility of TPR profile was confirmed by the iterative measurements at different temperatures. We attempted the same experiment on the CeO_2-Al_2O_3 catalyst. As described before, no oxidation at 773 K was observed because of the formation of stable $CeAlO_3$ after TPR up to 1273 K.

2.4. Estimation of OSC

The OSC of the CeO_2-ZrO_2 catalyst at 773 K was estimated by O_2 pulse injection. The catalyst placed in a reactor was reduced in flowing 10 vol.% H_2/Ar with the same heating rate of TPR. After reaching at 1273 K, the temperature was kept for 30 min, and then the catalyst was cooled to 773 K in a stream of He. The pulse of 5 ml of 1 vol.% O_2/He was injected at a regular interval until no more loss of O_2 injected was detected.

The consumption of oxygen at 773 K was observed by using an on-line gas chromatograph (Shimadzu GC-8A) equipped with a thermal conductivity detector (TCD).

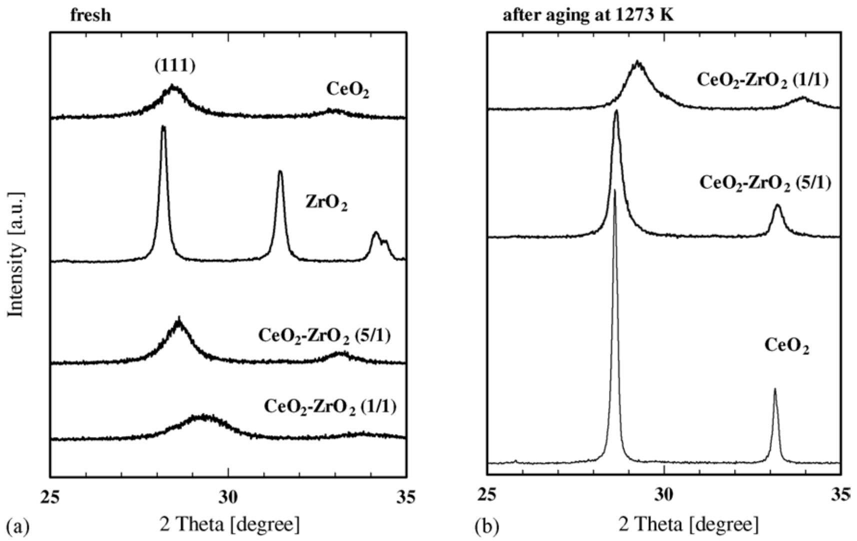

Fig. 1. X-ray diffraction patterns of CeO_2-ZrO_2 catalysts: (a) fresh and (b) after the aging at 1273 K for 1 h.

3. Results and discussion

3.1. Characterization of catalyst

X-ray diffraction measurements of catalysts calcined at 773 K and aged at 1273 K were carried out. Due to the detailed analysis concerning the formation of solid solution, the XRD patterns with the diffraction angle from 25° to 35° are presented in Fig. 1. In fresh catalysts (Fig. 1(a)), the first peaks of both CeO_2-ZrO_2 catalysts shift to higher angle with increasing CeO_2 content compared to the peak of CeO_2 itself, indicating the insertion of ZrO_2 into CeO_2 lattice, i.e. the formation of CeO_2-ZrO_2 solid solutions at 773 K. The XRD pattern of the CeO_2-ZrO_2(1/1) catalyst is attributed to $Ce_{0.5}Zr_{0.5}O_2$ but the structure of the CeO_2-ZrO_2(5/1) is not assigned clearly. When the catalysts were aged at 1273 K for 1 h, the sharp peaks, assigned to CeO_2, are detected on the CeO_2-ZrO_2(5/1) catalyst as shown in Fig. 1(b). The crystallization induced by the aging treatment is found pronouncedly on the CeO_2 as well as the CeO_2-ZrO_2(5/1) catalyst, suggesting that the presence of CeO_2 phase acts positively to promote the sintering. XRD peaks assigned to ZrO_2 are not detected in CeO_2-ZrO_2 catalysts.

As the catalysts were cyclically treated from room temperature to 1273 K for TPR measurements, changes in BET surface area and crystallite size are listed in Tables 1 and 2, respectively. The result shows that BET surface areas decrease drastically, while crystallite sizes increase with the decrease of BET surface areas. Therefore, the target catalysts to evaluate the oxidation behavior are the catalysts with low surface area and large crystallite size.

Table 1
BET surface area of CeO_2-ZrO_2 catalysts before and after the aging at 1273 K

	Fresh ($m^2 g^{-1}$)	1273 K for 1 h ($m^2 g^{-1}$)
CeO_2	130	5
CeO_2-ZrO_2(5/1)	103	13
CeO_2-ZrO_2(1/1)	30	5

Table 2
Crystallite size of CeO_2-ZrO_2 catalysts calculated from the first peak in Fig. 1

	Fresh (nm)	1273 K for 1 h (nm)
CeO_2	8	45
CeO_2-ZrO_2(5/1)	11	21
CeO_2-ZrO_2(1/1)	5	8

3.2. Oxidation behavior of catalysts

TPR spectra of CeO_2 are displayed in Fig. 2. TPR spectrum of fresh CeO_2 has two reduction peaks at 757 and

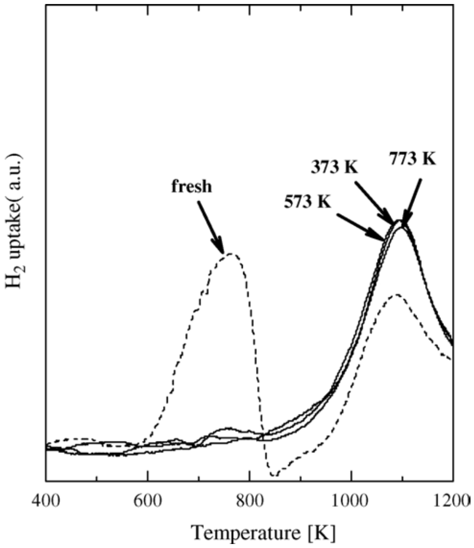

Fig. 2. TPR spectra of CeO_2. Temperatures in the figure means the temperatures carried out the consecutive oxidation for 1 h after TPR measurements.

1085 K, respectively. The first peak is due to the reduction of surface oxygen species adsorbed on CeO_2 because the first peak disappeared from TPR spectra after the consecutive oxidation. The second peak is attributed to the formation of Ce_2O_3. TPR spectra after the consecutive oxidation show only one peak at 1093 K and the peak areas are almost the same, even the oxidation at 373 K, suggesting that the amount of oxygen stored is independent on the oxidation temperatures when CeO_2 is reduced at 1273 K. This means that the reduced CeO_2 is very sensitive to oxygen as reported El Fallash et al. [21] and the same amounts of oxygen species reacted are reversibly consumed in the reductive atmosphere. In addition, the surface oxygen species, weakly adsorbed on CeO_2, do not exist and most of oxygen consume for the reaction with Ce^{3+} species. As given in Table 2, the crystallite size estimated is 45 nm and so large. The amount of active oxygen around 1000 K will be improved if the crystallite size can be kept to be small above 1000 K.

Fig. 3 shows TPR spectra of both CeO_2-ZrO_2 catalysts. The CeO_2-ZrO_2(1/1) catalyst provides TPR spectra with one peak as shown in Fig. 3a. The peak from the fresh catalyst appears at 844 K and is shifted to at 888 K after the consecutive oxidation. The peak areas decrease with decreasing the oxidation temperature although the peak positions are the same at 888 K. Assuming that the consumed oxygen in Fig. 3a is derived from the reduction of Ce^{4+} to Ce^{3+}, the oxidation activity is correlated with the stability of Ce^{3+} in the solid solution phase. Thus, the Ce^{3+} in the CeO_2-ZrO_2(1/1) catalyst is more stable than that in the reduced CeO_2.

On the other hand, the TPR profile of CeO_2-ZeO_2(5/1) catalyst is different from the CeO_2-ZrO_2(1/1) catalyst and CeO_2. The result displays in Fig. 3b. The profiles of the fresh catalyst and after the consecutive oxidation are almost the same: two reduction peaks around 863 K and at 1070 K. The similar TPR spectra are observed even after the consecutive oxidation at 373 K. This is the same oxidation behavior of CeO_2. The peak at 1070 K, attributed to the formation of Ce_2O_3, is shifted from 1083 K observed on CeO_2 (Fig. 2). The first peak around 863 K appears at the similar temperature observed on the CeO_2-ZrO_2(1/1) catalyst. TPR results suggest that the CeO_2-ZeO_2(5/1) catalyst contains two phases: one is a solid solution phase; the other is CeO_2, although XRD pattern of the CeO_2-ZeO_2(5/1) catalyst was assigned to CeO_2 (Fig. 1(b)). The solid solution phase acts effectively to form mobile oxygen species at lower temperatures and various solid solution phases presumably exist from the peak shape. Moreover, the reduction of CeO_2 phase becomes readily by the interaction of the solid solution phase, resulting in the lower reduction temperature than CeO_2 itself (Fig. 2).

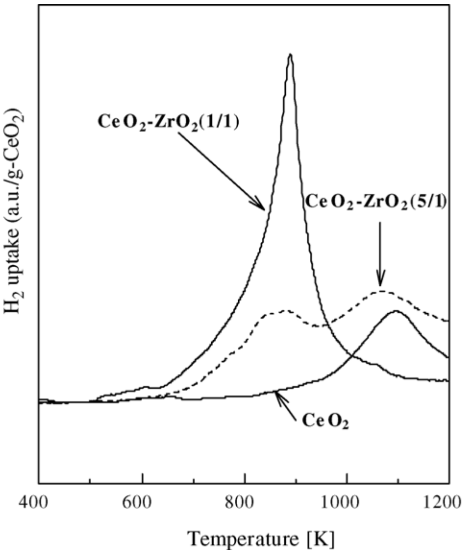

Fig. 4. TPR spectra of CeO_2-ZrO_2 catalysts after the consecutive oxidation at 773 K for 1 h.

Fig. 4 shows TPR spectra of those catalysts after the consecutive oxidation at 773 K, where the peak intensity is converted to "/g-CeO_2", for comparison. The reducibility corresponding to the amount of mobile oxygen species is enhanced by the formation of solid solutions. The positive effect on the solid solutions phase observed in this experi-

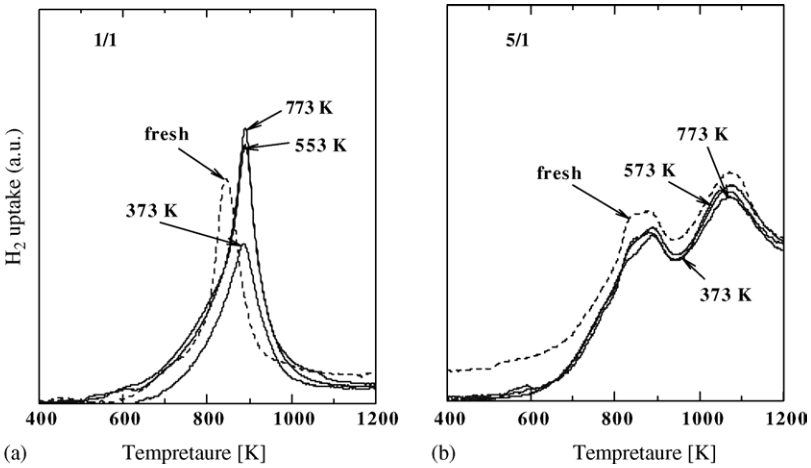

Fig. 3. TPR spectra of CeO_2-ZrO_2 catalysts: (a) CeO_2-ZrO_2(1/1) and (b) CeO_2-ZrO_2(5/1). Temperatures in the figure means the temperatures carried out the consecutive oxidation for 1 h after TPR measurements.

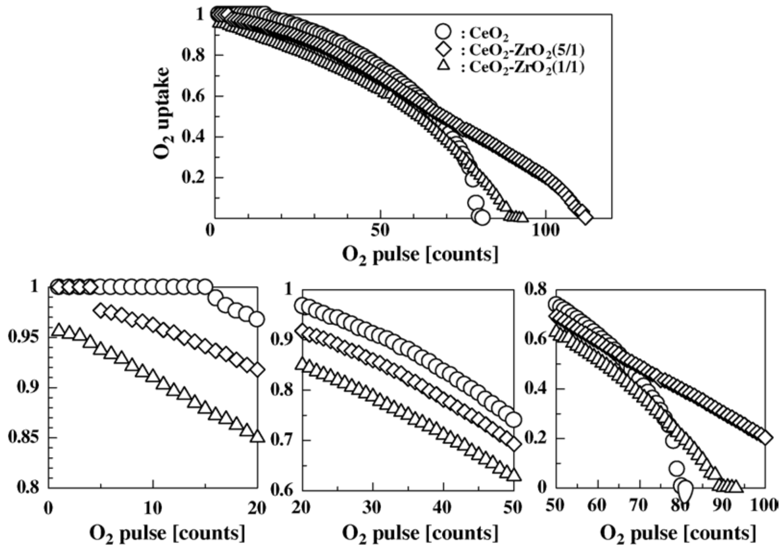

Fig. 5. O_2 consumption profiles of CeO_2-ZrO_2 catalysts. A pulse of 5 ml of 1 vol.% O_2/He was injected at 773 K after the reduction at 1273 K.

ment, i.e. the generation of a large number of mobile oxygen at low reduction temperatures, is consistent with others previously reported [10,17,22]. As the crystallite size of the solid solution contributes strongly to the generation of OSC [7], the next subject on the improvement of OSC is to attempt the preparation of thermally resisted CeO_2-ZrO_2 catalysts.

3.3. Estimation of OSC by O_2 pulse injection

Fig. 5 represents the oxidation behavior examined by means of the O_2 pulse injection at 773 K. The O_2 uptake is plotted as ordinate—1 indicates the storage of 100% O_2 in 5 ml of 1 vol.% O_2/He. The number of injected pulses until the saturation are 81 for CeO_2, 113 for the CeO_2-ZrO_2(5/1) catalyst and 93 for the CeO_2-ZrO_2(1/1) catalyst, respectively. The amounts of oxygen stored (OSC) are summarized in Table 3. The result is similar to those estimated by O_2 pulse injection [22–24] although they did not mention the number of O_2 pulse and the O_2 consumption profile as shown in Fig. 5. Assuming that Ce^{4+} species in CeO_2 are completely reduced to Ce^{3+} species, 250 mmol (mol-CeO_2)$^{-1}$ is the largest value. Thus, about 50% of Ce species in the CeO_2-ZrO_2(1/1) catalyst participates in the Ce^{3+}(1273 K)/Ce^{4+}(773 K) change. The amount of oxygen stored in the CeO_2-ZrO_2(1/1) catalyst is 1.5 times as large as CeO_2 itself. The order in Table 3 is well agreement with the result in Fig. 4, suggesting that the formation of solid solution phases assists the increase of mobile oxygen species, which are essential for the smooth catalytic operation of automotive catalysts. The profiles shown in Fig. 5a are reflected the oxidation behavior of surface and bulk on the catalysts. The oxidation by first a few O_2 pulses occurs only on the surface and next the bulk in the catalysts contributes to the oxidation. The bulk oxidation presumably is controlled by the diffusion rate of mobile oxygen at 773 K. Fig. 5a is divided into three parts: (1) O_2 pulse region of 0–20 in Fig. 5b; (2) O_2 pulse region of 20–50 in Fig. 5c; (3) O_2 pulse region above 50 in Fig. 5d. On CeO_2, oxygen in the pulse is consumed completely during the first 15 pulses and the number of pulses consumed completely decreases to four pulses on the CeO_2-ZrO_2(5/1) catalyst. However, on the CeO_2-ZrO_2(1/1) catalyst, only 95% of oxygen is consumed even at the first pulse. Therefore, the order of reactivity of Ce^{3+} is $CeO_2 > CeO_2$-ZrO_2 (5/1) > CeO_2-ZrO_2(1/1) and the Ce^{3+} species in the reduced CeO_2 phase are very sensitive to oxygen at 773 K. This is in good agreement with TPR result of CeO_2 itself. As the O_2 consumption is influenced by the surface concentration of Ce $^{+}$, the concentration decrease in the series of CeO_2, CeO_2-ZrO_2 (5/1), and CeO_2-ZrO_2(1/1), too. The high activity of the CeO_2-ZrO_2(5/1) catalyst indicates the presence of the reduced CeO_2 on the surface. Although it is difficult to distinguish between the surface oxidation and the bulk oxidation from the profiles, the analysis of change in the consumption rate of O_2 estimated from the profile is attempted. The consumption rate per pulse nonlinearly decreases with increasing O_2 pulse on the CeO_2-ZrO_2(1/1) catalyst. If Ce^{3+} species are distributed only on the surface, the oxidation rate will decrease linearly. The nonlinear profile gives the information with respect to the distribution of Ce^{3+} species in the reduced catalyst. Three kinds of consumption rates are speculated from the profile on the CeO_2-ZrO_2(1/1) catalyst. The rates might be the surface oxidation, the bulk oxidation at near surface and the bulk oxidation, respectively. In order to elucidate the oxidation behavior from the consumption rate, further investigations are necessary.

Table 3
OSC estimated from O_2 pulse injection at 773 K

	O_2 (mmol g^{-1})	O_2 (mmol (mol-CeO_2)$^{-1}$)
CeO_2	0.50	85
CeO_2-ZrO_2(5/1)	0.52	107
CeO_2-ZrO_2(1/1)	0.45	133

However, the analysis by O_2 pulse injection is very useful to characterize the surface concentration of Ce^{3+} formed on the catalyst, particularly, with both the same Ce/Zr ratio and the different preparation method. Because the oxygen injected is react only with Ce^{3+} species and the behavior of consumed oxygen is correlated with the distribution of Ce^{3+} on the surface. We believe that the oxidation profile measured by the O_2 pulse injection will help to understand the change in the oxidation activity on the catalyst prepared by either the same or the different methods. Further experiments are required to establish as the analytical technique on the CeO_2-ZrO_2 catalysts, too.

4. Conclusions

The oxidation behavior on the reduced CeO_2-ZrO_2 catalysts was evaluated. Ce^{3+} species formed from the CeO_2 phase were very sensitive to oxygen but Ce^{3+} species formed in the solid solutions were relatively stable. The formation of solid solution facilitated the reducibility of Ce^{4+} species at low temperature and the oxygen consumption per mol-CeO_2 was improved, too. It was presumed that the solid solution phase prevented the sintering at 1273 K and the resulting small crystallite size promoted effectively the increase of mobile oxygen estimated as OSC at 773 K. Finally, the O_2 pulse injection method was a useful technique to characterize the CeO_2-ZrO_2 catalyst because the distribution of Ce^{3+} species on and into the catalysts could be analyzed by the titration profiles.

References

[1] H.S. Gandhi, G.W. Graham, R.W. McCabe, J. Catal. 216 (2003) 433.
[2] T. Miki, T. Ogawa, M. Haneda, N. Kakuta, A. Ueno, S. Tateishi, S. Matsuura, M. Sato, J. Phys. Chem. 94 (1990) 6463.
[3] M. Haneda, T. Mizushima, N. Kakuta, A. Ueno, Y. Sato, S. Matsuura, K. Kasahara, M. Sato, Bull. Chem. Soc. Jpn. 66 (1993) 1279.
[4] M. Haneda, T. Mizushima, N. Kakuta, J. Chem. Soc. Faraday Trans. I 91 (1995) 4459.
[5] N. Kakuta, N. Morishima, M. Kotobiki, T. Iwase, T. Mizushima, Y. Sato, S. Matsuura, Appl. Surf. Sci. 121–122 (1997) 408.
[6] M. Haneda, T. Mizushima, N. Kakuta, J. Phys. Chem. B 102 (1998) 6579.
[7] M. Sugiura, Catal. Surveys Asia 7 (2003) 77.
[8] A. Trovarelli, Catalysis by Ceria and Related Materials, Imperial College Press, 2002.
[9] M. Ozawa, M. Kimura, A. Isogai, J. Alloys Compd. 193 (1993) 73.
[10] N. Hickey, P. Fornasiero, R. Di Montre, J. Kaspar, M. Graziani, G. Dolcetti, Catal. Lett. 72 (2001) 45.
[11] J. Kaspar, R. Di Monte, P. Fornasiero, M. Graziani, H. Bradshaw, C. Norman, Topics Catal. 16/17 (2001) 83.
[12] L.F. Liotta, A. Macaluso, G. Pantaleo, A. Longo, A. Martorana, G. Deganello, G. Marci, S. Gialanella, J. Sol–Gel Sci. Technol. 26 (2003) 235.
[13] T. Nakatani, T. Wakita, R. Ota, K. Tanaka, T. Wakasugi, J. Ceram. Soc. Jpn. 111 (2003) 137.
[14] T. Sasaki, Y. Ukyo, A. Suda, M. Sugiura, K. Kuroda, S. Arai, H. Saka, J. Ceram. Soc. Jpn. 111 (2003) 382.
[15] M. Alifanti, B. Blangenois, J. naud, P. Grange, B. Delmon, Chem. Mater. 15 (2003) 395.
[16] C.E. Hori, H. Permana, K.Y. Simon Ng, A. Brenner, K. More, K.M. Rahmoeller, D. Belton, Appl. Catal. B 16 (1998) 105.
[17] T. Masui, Y. Peng, K. Machida, G. Adachi, Chem. Mater. 10 (1998) 4005.
[18] V.S. Escribano, E.F. Lopez, M. Panizza, C. Resini, J.M.G. Amores, G. Busca, Solid State Sci. 5 (2003) 1369.
[19] P. Fornasiero, J. Kaspar, T. Montini, M. Graziani, V.D. Santo, R. Oasaro, S. Recchina, J. Mol. Catal. A 204-205 (2003) 683.
[20] A. Martorana, G. Deganello, A. Longo, A. Prestianni, L. Liotta, A. Macaluso, G. Pantaleo, A. Balerna, S. Mobilio, J. Solid State Chem. 177 (2004) 1268.
[21] J. El Fallash, S. Boujana, H. Dexpert, A. Kiennemann, J. Majerus, O. Touret, F. Villain, F. Le Normand, J. Phys. Chem. 98 (1994) 5522.
[22] C. de Leitenburg, A. Trovarelli, F. Zamar, S. Maschio, G. Dolcetti, J. Llorca, J. Chem. Soc. Chem. Commun. (1995) 2181.
[23] P. Fornasiero, G. Balducci, R. Di Monte, J. Kaspal, V. Sergo, G. Gubitosa, A. Ferrero, M. Graziani, J. Catal. 164 (1996) 173.
[24] P. Vidmar, P. Fornasiero, J. Kaspal, G. Gubitosa, M. Graziani, J. Catal. 171 (1997) 160.